Collective vibrations of an α-helix
A molecular dynamics study

Jürgen Pleiss and Fritz Jähnig
Max-Planck-Institut für Biologie, D7400 Tübingen, Federal Republic of Germany

ABSTRACT The internal dynamics of a 20-residue polyalanine helix was investigated by molecular dynamics simulations. Special attention was paid to the collective vibrations of the helix backbone. The stretch and bend vibrations could be assigned unambiguously to oscillations with periods of 1.4 and 4.3 ps, respectively. The influence of the environment on the dynamics of the collective vibrations was studied by coupling the helix to a heat bath and by adding water molecules. In the presence of water, the stretch vibration becomes more strongly damped, but still exists as a vibration, while the bend vibration becomes overdamped and degenerates into a relaxation process. The results are compared with available experimental data.

INTRODUCTION

It is by now an accepted fact that proteins are not rigid structures but dynamic entities able to undergo structural changes (for a recent review see reference 1). These changes range from atomic fluctuations in the femtosecond range up to conformational changes in the range of seconds. Conformational changes are involved in enzymatic activity and, therefore, are agreed to be functionally relevant. Fluctuations in the femtosecond and picosecond range, however, have long been questioned as being relevant for protein activity. It is only in the last few years that data have been presented indicating that actually the fast fluctuations are the origin of the slow conformational changes (2, 3). A hierarchical order has been postulated for the relation between the different kinds of motions (2). Fast thermal fluctuations give rise to slower ones, which cause still slower ones, until finally a conformational change occurs. Hence, fast internal fluctuations appear to be relevant to protein activity.

Several different experimental techniques have been applied to study fast internal fluctuations of proteins, among them Raman (4, 5) and infrared (6) spectroscopy, microwave absorption (7), inelastic neutron scattering (8), fluorescence anisotropy decay (3, 9), Möβbauer spectroscopy (10), and nuclear magnetic resonance (11). Theoretical techniques which have contributed to increase the understanding of the internal dynamics of proteins involve normal mode analysis (12, 13) and molecular dynamics simulations (14).

For the present studies we used the molecular dynamics (MD) technique. With this technique a time range up to some hundreds of picoseconds is accessible with present-day computers. Even in this limited time range, however, it is not yet clear whether the temporal behavior of proteins is described correctly by MD (15, 16). The localized oscillations of bond lengths and angles which occur in the femtosecond range are treated correctly, but this is not astonishing because spectroscopic data have been used to determine the parameters of the bonded interactions (17). Slower delocalized or collective oscillations such as stretch or bend vibrations of helices which occur in the picosecond range have been observed in MD simulations on proteins (18, 19) and peptides (20, 21), but were not tested against experimental data. Still slower modes in the range of hundreds of picoseconds such as the diffusive reorientation of side chain rings turned out as too fast in MD simulations compared to experimental data (22).

Two reasons for this failure are conceivable. First, the description of the nonbonded interactions within the proteins may be inadequate and, second, the interactions of the proteins with the solvent may be treated incompletely. Of the internal nonbonded interactions, especially the electrostatic interaction is still under debate (23, 24). Concerning interactions with the solvent, water has recently been shown to have a considerable effect on the internal dynamics of a protein (25).

To investigate these two possible error sources in more detail, we performed MD simulations on a 20-residue polyalanine helix. This peptide is small enough to permit simulations over an extended time range and large enough to adopt an α-helical structure (26). Spectroscopic data on the internal vibrations are also available (4–6). These vibrations range from fast localized bond vibrations to slower delocalized collective vibrations such as stretch and bend vibrations of the helix. The MD result obtained is in good agreement with the experimental data, especially for the stretch vibra-

0006-3495/91/04/795/10 $2.00

tion. This lends support to the description of the interactions used in the MD simulations, including the nonbonded interactions.

The influence of the solvent on the internal dynamics of the helix was studied by introducing different kinds of coupling of the helix to the environment. In the simplest case, any coupling was omitted with the consequence that the temperature did not remain constant. In the second case, the helix was coupled to a heat bath in order to keep the temperature constant (27). Finally, in the third case, the helix was embedded into 570 water molecules. In each case, the internal dynamics of the helix was analyzed with special care devoted to the stretch and bend vibrations. A strong influence of the environment on the damping of these vibrations was observed, while the frequencies of the vibrations were hardly affected. Most pronounced was the effect on the bend vibration of the helix which in the presence of water became overdamped.

METHODS

MD simulations

For initial conformations a regular helix was generated with the backbone dihedrals ϕ, ψ set equal to $-57°$, $-47°$, and all peptide bonds in *trans*. When water molecules were included explicitly, the helix was placed in the center of a box of size $2 \times 2 \times 4.7$ nm filled with 570 water molecules, and periodic boundary conditions were applied.

Initial conformations were energy-minimized by the method of steepest descent. For this and the ensuing MD simulation the program Gromos (W. F. van Gunsteren and H. J. C. Berendsen, BIOMOS B. V., University of Groningen, Groningen, Netherlands) was used. The MD simulations were performed on a μVAX II and a CRAY-XMP.

All simulations were started with a heating period of 2 ps in which the temperature of the system was increased to 300 K under strong coupling to a heat bath. After this period, the system was in equilibrium as judged by the potential energy. The bond lengths were constrained by the SHAKE algorithm (28). Then the potential energy is a sum of terms involving bond angles, dihedrals, improper dihedrals, and terms describing the nonbonded electrostatic and Lennard-Jones interactions (29). The electrostatic interaction is calculated by taking into account only neutral charge groups and a dielectric constant of one. For the simulation with an explicit hydrogen bond interaction, an additional 10–12 potential was introduced (29). For all nonbonded interactions a cutoff of 1 nm was used with the neighbor list updated every 10 time steps. The time step was chosen as 2 fs. Coordinates were stored routinely at every 10 time steps, in some simulations at each time step.

To couple the helix to an external heat bath without explicitly simulating solvent molecules, an algorithm of Berendsen et al. (27) was adopted. After each integration step, the temperature of the helix is calculated from the velocities of the atoms. If it deviates from 300 K, the velocities are rescaled with a relaxation time τ. Formally, the relaxation time is inversely proportional to the viscosity of the surrounding solvent, hence, a small relaxation time corresponds to a highly viscous solvent. Three values for τ were used: $\tau = 9{,}000$ ps for no coupling, $\tau = 100$ fs for weak coupling, and $\tau = 10$ fs for strong coupling.

Helix length and bend angle

If the length of a helix is calculated as the distance between two atoms at both ends of the helix, all the local fluctuations of the two atoms are reflected by the length. To eliminate this effect, the helix length was calculated as the distance between two groups of atoms at the NH_2- and COOH-terminus. We determined the centers of mass of the backbone atoms of Ala2–Ala5 and Ala16–Ala19, and used their distance l as a measure for the helix length. It is smaller than the end-to-end distance, therefore, only relative changes were compared, $(l - \langle l \rangle)/\langle l \rangle$, with $\langle l \rangle$ denoting the temporal average.

In a similar way, the bend angle θ of the helix was calculated as the angle between the axes $\vec{n}_1$ and $\vec{n}_2$ of the NH_2- and COOH-terminal segments. The axes $\vec{n}_1$ and $\vec{n}_2$ were determined by adding the unit vectors between the atom pairs N3–C_α6, C_α3–C6, C3–N7, N4–C_α7, C_α4–C7, C4–N8, and the atom pairs C11–N15, N12–C_α15, C_α12–C15, C12–N16, N13–C_α16, C_α13–C16, respectively.

Correlation functions

To analyze the dynamic behavior of the helix appropriate correlation functions were calculated. They are defined as temporal averages (30),

$$C_x(t) = \langle \Delta x(t') \, \Delta x(t' + t) \rangle$$

$$= \lim_{T \to \infty} \frac{1}{T} \int_0^T \Delta x(t') \, \Delta x(t' + t) \, dt', \quad (1)$$

with $\Delta x(t) = x(t) - \langle x \rangle$ denoting the displacement of the quantity $x(t)$ from its temporal average $\langle x \rangle$. At time zero, $C_x(0) = \langle (\Delta x)^2 \rangle$, the mean-square displacement, and at long times $C_x(\infty) = 0$.

Especially when the quantity x oscillates, it is advantageous to study the Fourier transform of its correlation function

$$\tilde{C}_x(\omega) = \lim_{T \to \infty} \int_0^T C_x(t) e^{i\omega t} \, dt. \quad (2)$$

Because in the numerical calculation the time interval T for the integration is finite, the Fourier transform $\tilde{C}_x(\omega)$ is defined only at frequencies $\omega = 2\pi n/T$, with n integer. Often instead of the angular frequency ω the frequency $\nu = \omega/2\pi$ is used or the corresponding wavenumber $\bar{\nu} = \nu/c$, with c denoting the velocity of light.

The quantity x may be the position of an atom, a dihedral angle, or the length or bend angle of the helix. If x is a vector like the position $\vec{x}$ of an atom, the scalar product is taken to calculate $C_x(t)$. Sometimes temporal derivatives ordinary $v = \mathrm{d}x/\mathrm{d}t$ of these quantities are used, e.g., the velocity of an atom with $\vec{v} = \mathrm{d}\vec{x}/\mathrm{d}t$. The information contained in C_v is the same as in C_x. This is especially obvious from their Fourier transforms, because

$$\tilde{C}_v(\omega) = \omega^2 \tilde{C}_x(\omega). \quad (3)$$

However, the high-frequency motions are weighted more strongly in $\tilde{C}_v(\omega)$. Hence, for their analysis it is preferable to use $\tilde{C}_v(\omega)$, whereas for the low-frequency motions $\tilde{C}_x(\omega)$ is preferable.

Harmonic oscillator model

A harmonic oscillator in contact with a heat bath may be described by the Langevin equation (30, 31)

$$m \frac{\mathrm{d}^2 x}{\mathrm{d}t^2} + m\beta \frac{\mathrm{d}x}{\mathrm{d}t} + \mathrm{grad}\, V = A(t). \quad (4)$$

Here, m is the mass of the oscillating particle, β the damping

coefficient (sometimes called friction coefficient), $V = 1/2\ m\omega_0^2 x^2$ the harmonic potential, and $A(t)$ the stochastic force giving rise to thermal fluctuations. In the case $\omega_0 > \beta/2$, the oscillator is periodic, in the case $\omega_0 < \beta/2$ it is overdamped. The displacement and velocity autocorrelation functions for such an oscillator have been calculated (31). In the limit $\omega_0 \gg \beta/2$, they are given by

$$C_x(t) = \langle x^2 \rangle \exp(-\beta t/2) \cos(\omega_0 t) \quad (5)$$

$$C_v(t) = \langle v^2 \rangle \exp(-\beta t/2) \cos(\omega_0 t), \quad (6)$$

and in the limit $\omega_0 \ll \beta/2$ by

$$C_x(t) = \langle x^2 \rangle \exp(-\omega_0^2 t/\beta) \quad (7)$$

$$C_v(t) = \langle v^2 \rangle \exp(-\beta t). \quad (8)$$

The Fourier transforms of the autocorrelation functions are, for both cases $\omega_0 > \beta/2$ and $\omega_0 < \beta/2$,

$$\tilde{C}_x(\omega) = \frac{kT}{m} \frac{\beta}{(\omega_0^2 - \omega^2)^2 + \beta^2 \omega^2} \quad (9)$$

and $\tilde{C}_v(\omega) = \omega^2 \tilde{C}_x(\omega)$.

Elastic rod model

The properties of an isotropic elastic rod are determined by its elasticity modulus Y (32). For a rod with free ends, the frequencies of the stretch and bend vibrations result as

$$\nu^{(s)} = \frac{1}{2L} (Y/\rho)^{1/2} \quad (10)$$

and

$$\nu^{(b)} = 1.12 \frac{R}{L^2} (Y/\rho)^{1/2}, \quad (11)$$

with ρ denoting the density of the rod, R the radius, and L the length. For a helix of 20 alanine residues, one may assume $L = 3$ nm, $R = 0.45$ nm, and $\rho = 1.24$ g/cm^3. The ratio $\nu^{(s)}/\nu^{(b)}$ is independent of Y, and with these numbers for a helix becomes $\nu^{(s)}/\nu^{(b)} = 3.0$.

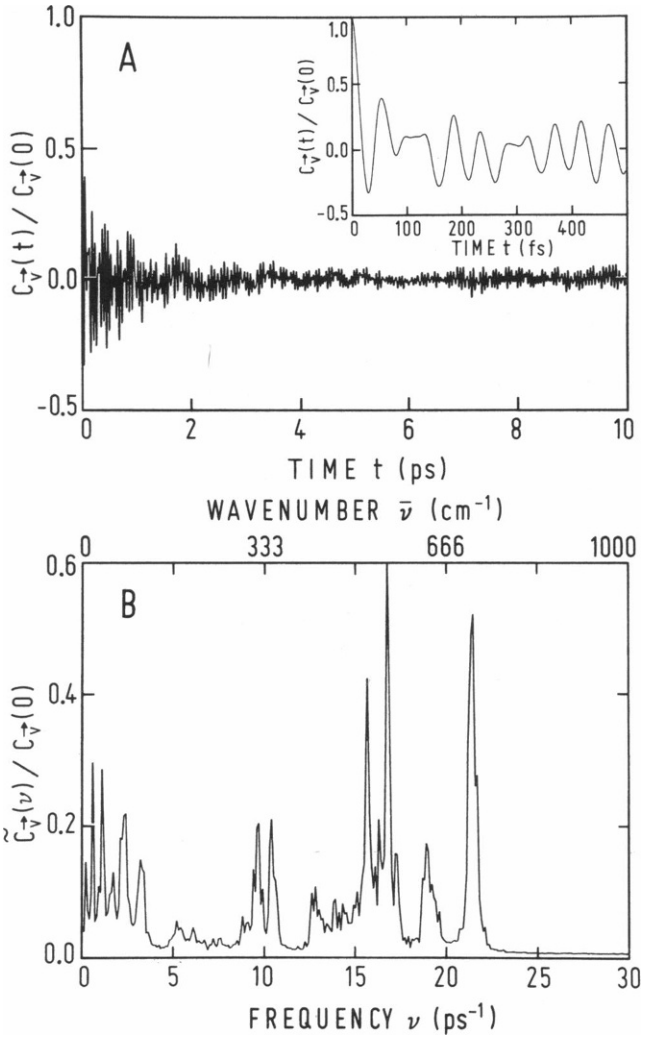

FIGURE 1 Velocity autocorrelation function $C_v(t)$ for C_α11 of an $(Ala)_{20}$-helix obtained from a 160 ps trajectory with an output at every 2 fs (A), and its Fourier transform $\tilde{C}_v(\nu)$ derived from the time range 0–10 ps (B). The inset in A shows the first 500 fs on an extended time scale. The helix was weakly coupled to a heat bath at 300 K.

RESULTS AND DISCUSSION

Atomic fluctuations

The fluctuations of individual atoms were investigated by calculating their velocity autocorrelation function $C_v(t)$. Fig. 1 A shows this function for the C_α atom of Ala11, a residue in the middle of the $(Ala)_{20}$-helix. The helix was weakly coupled to a heat bath at 300 K to keep the temperature constant. For other backbone atoms, similar results were obtained. After a rapid initial decay which occurs within 10–20 fs, $C_v(t)$ exhibits damped oscillations with a period of ~60 fs. In addition, there is a weak indication of an oscillation with a period of ~1 ps.

In the Fourier transform $\tilde{C}_v(\nu)$ shown in Fig. 1 B, the 60 fs oscillation appears as a peak at $\nu = 17$ ps^{-1}, corresponding to a wavenumber $\bar{\nu} = 560$ cm^{-1}. In addition, there are other peaks in the range of 8–22 ps^{-1} (260–730 cm^{-1}) and 0–3 ps^{-1} (0–100 cm^{-1}). If the bond lengths are not kept constant by the SHAKE algorithm, essentially the same spectrum in the range up to 25 ps^{-1} is obtained, whereas at higher frequencies new peaks appear due to bond length vibrations. These results are in fair agreement with experimental data on polyalanine from Raman spectroscopy (4) and with the results of a normal coordinate analysis (13).

The fast initial decay of $C_v(t)$ reflects the relaxation of the atomic velocities to a Maxwell distribution and has already been observed in other cases (16, 25). Oscilla-

tions with a period of 60 fs were also found in the autocorrelation function of the bond and dihedral angles of the helix backbone (data not shown) and, therefore, are interpreted as orginating from oscillations of bond and dihedral angles.

To analyze the slow oscillations with a period of ~1 ps, it is advantageous to employ the displacement autocorrelation function $C_{\tilde{x}}(t)$. For the C_α atom of Ala11, this function is shown in Fig. 2 *A*. It was normalized by its value at time zero, $C_{\tilde{x}}(0) = \langle(\Delta\tilde{x})^2\rangle = 0.3$ Å^2. This value for the mean-square displacement is typical for C_α atoms of peptides or proteins (19, 20). Included in Fig. 2 *A* is the displacement autocorrelation function for the C_α atom of Ala1. Both functions exhibit oscillations with a period of ~5 ps. In the Fourier transforms $\tilde{C}_{\tilde{x}}(\nu)$ shown in Fig. 2 *B*, these oscillations give rise to a peak at ~0.2 ps^{-1}, corresponding to a wavenumber of 7 cm^{-1}. These slow oscillations may tentatively be assigned to collective vibrations of the helix. It is not possible at this stage, however, to distinguish between the two collective vibrations of a helix, the stretch and bend vibrations. This requires a more detailed analysis as presented in the following paragraph.

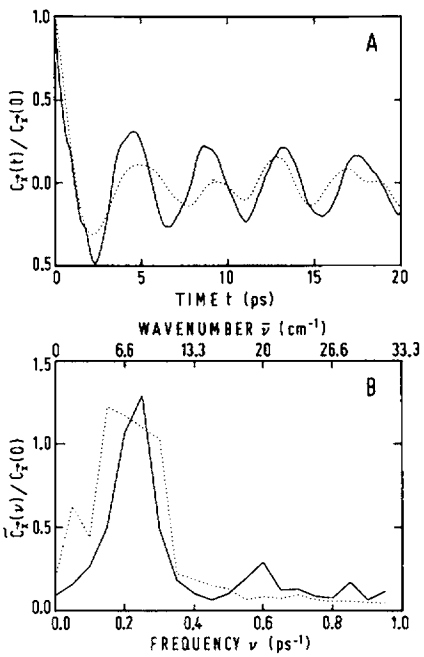

FIGURE 2 Displacement autocorrelation functions $C_{\tilde{x}}(t)$ for C_α11 (——) and C_α1 (· · ·) as obtained from a 400 ps trajectory with an output at every 20 fs (*A*), and their Fourier transforms $\tilde{C}_{\tilde{x}}(\nu)$ derived from the time range 0–20 ps (*B*). The helix was weakly coupled to a heat bath at 300 K.

Collective vibrations of the helix

To analyze the stretch vibrations of the helix, we determined the centers of mass of two groups of atoms at the two ends of the helix and used their distance l as a measure for the helix length. This distance is somewhat smaller than the end-to-end helix length, but for the analysis of the oscillations this does not matter. Fig. 3 *A* shows this reduced helix length l as a function of time. It

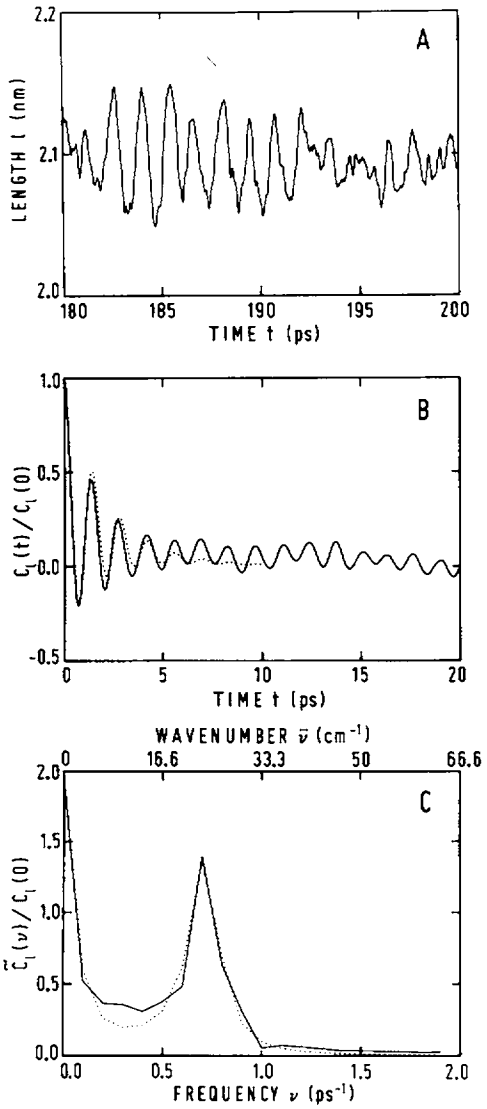

FIGURE 3 Length $l(t)$ of the $(Ala)_{20}$-helix (*A*), the length autocorrelation function $C_l(t)$ as obtained from a 400 ps trajectory (*B*), and its Fourier transform $\tilde{C}_l(\nu)$ derived from the time range 0–10 ps (*C*). The Fourier transform was fitted by the sum of two terms describing damped harmonic oscillators according to Eq. 9 (· · ·). The fit parameters were used to calculate the corresponding autocorrelation function (· · ·) in time (*B*). The helix was weakly coupled to a heat bath at 300 K.

performs oscillations with a period of 1.4 ps and a root-mean-square (rms) amplitude $\langle(\Delta l)^2\rangle^{1/2} = 0.26$ Å corresponding to 1.3% of the average length $\langle l \rangle$. The length autocorrelation function $C_l(t)$ is shown in Fig. 3 *B* and exhibits oscillations with the same period. The amplitude of the oscillations decreases rapidly during the first 5 ps, but thereafter the decrease is much slower.

The oscillations in $C_l(t)$ at long times arise from oscillations of the helix length over several periods without appreciable damping (Fig. 3 *A*). Outside such regions, the oscillations of the length are more stochastic, i.e., more strongly damped, giving rise to the oscillations in $C_l(t)$ at short times with their rapidly decreasing amplitude. Both types of correlations may be described by damped harmonic oscillators. To analyze the short-time correlations, we performed a Fourier transformation of $C_l(t)$ within the time range 0–10 ps and obtained a curve $\tilde{C}_l(\nu)$ with one peak at a finite frequency and another one at zero frequency (Fig. 3 *C*). The peak at finite frequency describes damped oscillations, the stretch vibrations of the helix, and the peak at zero frequency an overdamped relaxation of the helix length, which may tentatively be assigned to the effect of helix bending on the helix length. The spectrum was fitted by the sum of two displacement autocorrelation functions for damped harmonic oscillators, Eq. 9. For the peak at finite frequency we obtained the eigen frequency $\nu_0 = 0.73$ ps^{-1} and the damping coefficient $\beta = 0.80$ ps^{-1}, and for the peak at zero frequency the relaxation rate $\omega_0^2/\beta = 0.36$ ps^{-1}. The autocorrelation function in time corresponding to this superposition of two damped harmonic oscillators is included in Fig. 3 *B*. The short-time behavior of $C_l(t)$ is well described by the harmonic oscillator model, but the sustained oscillations in $C_l(t)$ at longer times, say after 5 ps, are not. They might be described by a third harmonic oscillator with the same frequency $\nu_0 = 0.73$ ps^{-1} but a much smaller damping coefficient β. The two oscillators might then be interpreted as two different substates of the helix (2). In both substates the helix would undergo stretch vibrations, but with different damping coefficients.

To study the influence of the hydrogen bonds on the stretch vibration, a simulation was performed with hydrogen bonds explicitly taken into account by an additional term in the interaction energy. The eigen frequency ν_0 of the stretch vibration increased by 40% (Table 1) and its amplitude decreased by 20%.

Spectroscopic data for the vibrations of long polyalanine helices have been analyzed previously within the framework of a normal coordinate analysis, and the wavenumbers for the stretch vibration of polyalanine helices of arbitrary length have been deduced (33). For an $(Ala)_{20}$-helix two different sets of experimental data

TABLE 1 **Frequencies ν_o of the stretch and bend vibrations of an $(Ala)_{20}$-helix**

Method	$\nu_o^{(s)}$	$\nu_o^{(b)}$
	ps^{-1}	ps^{-1}
Calculated without explicit H bonds	0.73	0.23
Calculated with explicit H bonds	1.06	0.33
Experimental (reference 33)	0.69 1.26	

yield 23 and 42 cm^{-1} corresponding to frequencies of 0.69 and 1.26 ps^{-1} (Table 1). These numbers are compatible with our MD result, their spread is even larger than the difference between the two values obtained with and without an explicit potential for hydrogen bonds. For the rms amplitude of the stretch vibration, the analysis of the spectroscopic data yielded 1.4% (33), in good agreement with our result.

To analyze the bend vibrations of the helix, the directions of two segments at the two ends of the helix were determined and the angle between them used as the bend angle θ of the helix. Inspection of helices with a finite θ on a graphics system indicated that the bend extends more or less homogeneously along the helix. Fig. 4 shows the autocorrelation function $C_\theta(t)$ of the bend angle exhibiting damped oscillations. A fit of the Fourier transform $\tilde{C}_\theta(\nu)$ (data not shown) by the expression for a damped harmonic oscillator yielded $\nu_0 = 0.23$ ps^{-1} and $\beta = 0.11$ ps^{-1}. Thus, the bend vibration is a factor of three slower than the stretch vibration (Table 1) and its damping coefficient is a factor of seven smaller.

One might have attempted to analyze the stretch vibrations of the helix by using the distance between two

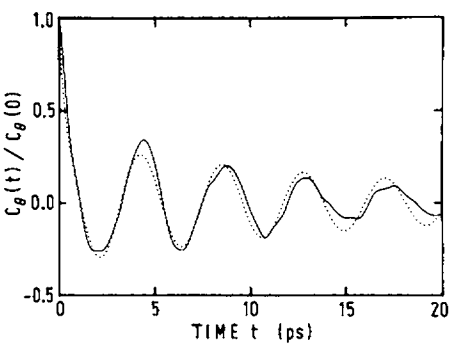

FIGURE 4 Autocorrelation function $C_\theta(t)$ of the bend angle $\theta(t)$ of the $(Ala)_{20}$-helix as obtained from a 400 ps trajectory. The curve was fitted as described in the legend to Fig. 3 (· · ·). The helix was weakly coupled to a heat bath at 300 K.

single atoms at the two ends of the helix as a measure for the helix length (18, 21). The corresponding autocorrelation function is shown in Fig. 5. It exhibits oscillations with a period of ~5 ps, superimposed on oscillations with a period of ~1 ps. Hence, both the stretch and the bend vibration are reflected in the distance between two single atoms. However, it is not possible from such an analysis to individually assign the stretch and the bend vibration to the two oscillations at 1.4 and 4.3 ps.

The ratio of the frequencies for the stretch and bend vibrations results as 4.3/1.4 = 3.1. This is the value expected if the helix behaves as an isotropic elastic rod (see Methods). Using Eqs. 14 and 15 and the numerical values for the stretch and bend vibrations, the elasticity modulus of the polyalanine helix is obtained as $Y^{(s)} = 2.1 \cdot 10^{11}$ dyn/cm^2 and $Y^{(b)} = 2.3 \cdot 10^{11}$ dyn/cm^2, respectively. These values are compatible with the value $(1.7–4.8) \cdot 10^{11}$ dyn/cm^2 calculated previously for a $(Gly)_{10}$-helix by a normal coordinate analysis (13). Lacking other data, our result may be compared with experimental values for the elasticity modulus of collagen helices determined as $(1.5–2) \cdot 10^{11}$ dyn/cm^2 by Brillouin scattering (34) and as $(3–5) \cdot 10^{11}$ dyn/cm^2 by measurement of the persistence length (35). Although the collagen helices differ from our regular α-helix, the values for the elasticity modulus lie in the same range.

Different environments

The MD simulations discussed above were performed on an $(Ala)_{20}$-helix under weak coupling to a heat bath at 300 K. To study the influence of the environment on the collective vibrations of the helix, three further kinds of coupling to the environment were investigated: (*a*) no coupling, (*b*) strong coupling to a heat bath at 300 K, and (*c*) coupling to 570 surrounding water molecules kept at 300 K.

To characterize thermodynamically the systems studied under the different conditions, the mean potential and kinetic energies of the helix and their rms fluctuations were calculated and are presented in Table 2 for weak and strong coupling to a heat bath and for coupling to water. For weak coupling, the potential energy fluctuates with an amplitude of ±22 kJ/mol around a mean value of zero. The kinetic energy fluctuates with an amplitude of ±18 kJ/mol around a mean value of ~300 kJ/mol. This mean value is expected for a canonical system of 123 atoms with fixed bond length at 300 K. Hence, one might conclude that the helix behaves as a canonical ensemble. This would imply that the potential and kinetic energies are uncorrelated and the fluctuations of the total energy are given by the sum of the fluctuations of the potential and kinetic energy, $\langle \Delta E^2_{tot} \rangle_{canonical} = \langle \Delta E^2_{pot} \rangle + \langle \Delta E^2_{kin} \rangle$. Insertion of numbers for $\langle \Delta E^2_{pot} \rangle$ and $\langle \Delta E^2_{kin} \rangle$ yields $\langle \Delta E^2_{tot/canonical} \rangle^{1/2} = \pm 28$ kJ/mol. This is about twice the actual value of $\langle \Delta E^2_{tot} \rangle^{1/2}$ obtained by first calculating the total energy as $E_{tot} = E_{pot} + E_{kin}$ and then its fluctuations. For a microcanonical ensemble, on the other hand, one would expect $\langle \Delta E^2_{tot} \rangle_{microcanonical} = 0$, i.e., the potential and kinetic energy would be perfectly anticorrelated. Hence, the helix coupled weakly to a heat bath behaves as a system somewhere between a canonical and a microcanonical ensemble, and the same is true for strong coupling to a heat bath and for coupling to water. This deficiency is partially a consequence of the algorithm used to describe the coupling to a heat bath. However, two additional sources of error have been proposed and would explain the deviation from a canonical ensemble even in the case of coupling to water: the inaccuracy of the integration algorithm and the introduction of a cutoff radius (27). In the case of no coupling of the helix to the environment, the potential and kinetic energies and with them the total energy increased continuously, as observed previously (27). This drift of the energy was the reason to introduce the coupling to a heat bath.

The autocorrelation functions $C_l(t)$ of the helix length for the different cases of coupling the helix to the environment are shown in Fig. 6. Without any coupling, the stretch vibrations are well pronounced, the initial decrease extends up to 10 ps and thereafter long-time correlations exist as in the case of weak coupling to a heat bath. The Fourier transform $\tilde{C}_l(\nu)$ was calculated using a time window of 10 ps and fitted by the sum of two terms describing damped harmonic oscillators, Eq. 9. The result for the oscillating term is presented in Table 3. The eigen frequency ν_0 of the oscillator is the same as for the case of weak coupling to a heat bath, but the damping coefficient β is smaller by a factor of 1.4. In the case of strong coupling to a heat bath, the amplitude of the oscillations in $C_l(t)$ decreases more rapidly than for weak coupling, and the amplitude of the superimposed relaxation is increased. The long-time correlations are

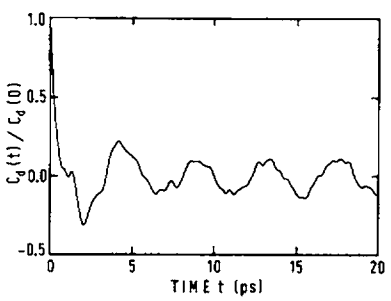

FIGURE 5 Autocorrelation function $C_d(t)$ of the helix length determined as the distance $C_\alpha 3$–$C_\alpha 18$, obtained from a 400 ps trajectory. The helix was weakly coupled to a heat bath at 300 K.

TABLE 2 **Mean values and rms deviations of the potential, kinetic, and total energies of an $(Ala)_{20}$-helix for three different couplings of the helix to the environment**

Coupling	$\langle E_{pot} \rangle$	$\langle E_{kin} \rangle$	$\langle E_{tot} \rangle$	$\langle \Delta E_{pot}^2 \rangle^{1/2}$	$\langle \Delta E_{kin}^2 \rangle^{1/2}$	$\langle \Delta E_{tot}^2 \rangle^{1/2}$
	kJ/mol	*kJ/mol*	*kJ/mol*	*kJ/mol*	*kJ/mol*	*kJ/mol*
Weak coupling to heat bath	−9	297	288	22	18	12
Strong coupling to heat bath	16	298	314	37	13	36
Coupling to water	14	304	318	26	20	24

more complex. Therefore, a time window of 5 ps was used to calculate the Fourier transform $\tilde{C}_l(\nu)$. A fit by the sum of two terms describing damped harmonic oscillators yielded for the oscillating term a slightly lower eigen frequency and a damping coefficient three times higher than for weak coupling to a heat bath (Table 3). If the helix is surrounded by water molecules, the stretch vibration is also strongly damped as expressed by the rapid decay of the autocorrelation function $C_l(t)$. The long-time correlations are more regular than for strong coupling to a heat bath and resemble those for weak coupling. A fit of the Fourier transform $\tilde{C}_l(\nu)$ calculated for a time window of 5 ps yielded roughly the same eigen frequency as for weak coupling and a damping coefficient β about twice as large.

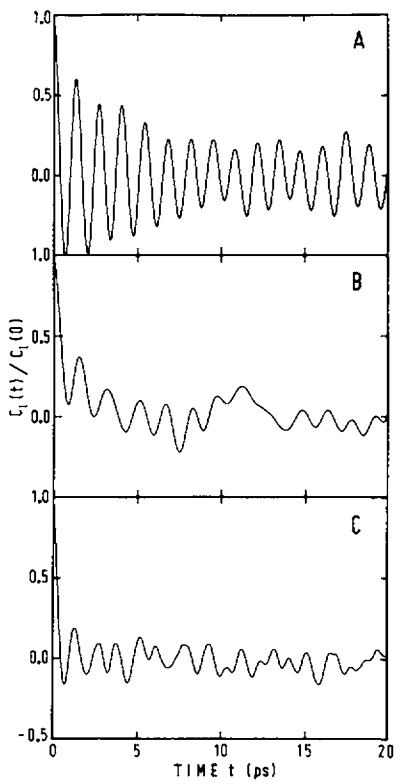

FIGURE 6 Autocorrelation functions $C_l(t)$ of the helix length for different cases of coupling the helix to the environment: no coupling (*A*), strong coupling to a heat bath at 300 K (*B*), and surrounded by 570 water molecules at 300 K (*C*). The curves were obtained from trajectories extended over 40 ps (*A*), 400 ps (*B*), and 60 ps (*C*).

The autocorrelation functions $C_\vartheta(t)$ of the helix bend angle for the different cases of coupling the helix to the environment are shown in Fig. 7. Without any coupling, the bend oscillations are well pronounced and weakly damped. For the case of strong coupling to a heat bath, the autocorrelation function rapidly decays to zero and provides only a very weak indication of a 5 ps oscillation. Obviously, the bend vibration has become overdamped. The same is true for the case of coupling to water. The decay of the autocorrelation function is less rapid, but the 5 ps oscillations are even less pronounced. The damping coefficient may be estimated by fitting the autocorrelation function by the expression for a harmonic oscillator in the overdamped case, Eq. 7. Using the time range 0–10 ps for the fit, one obtains for the relaxation time $\omega_0^2/\beta = 0.2\ ps^{-1}$. Under the assumption that the angular frequency $\omega_0 = 1.5\ ps^{-1}$ of the bend vibration is not altered by the presence of water, the damping coefficient results as $\beta = 11\ ps^{-1}$. Hence, the condition for overdamping, $\omega_0 < \beta/2$, is fulfilled. Sur-

TABLE 3. **Results of fits of the Fourier transform $\tilde{C}_l(\nu)$ of the displacement autocorrelation function for the helix length by the sum of two terms describing damped harmonic oscillators**

Coupling	ν_0	β	$\langle (\Delta l)^2 \rangle^{1/2} / \langle l \rangle$
	ps^{-1}	ps^{-1}	
No coupling*	0.70	0.56	0.014
Weak coupling to heat bath*	0.73	0.80	0.013
Strong coupling to heat bath‡	0.69	2.4	0.022
Coupling to water‡	0.83	2.0	0.012

The values for the eigen frequencies ν_0 and the damping coefficients β of the stretch vibration are presented for four different cases of coupling of the helix to the environment. The relative rms fluctuations $\langle (\Delta l)^2 \rangle^{1/2} / \langle l \rangle$ of the length are included. *The time window for the Fourier transformation was 10 ps. ‡The time window for the Fourier transformation was 5 ps.

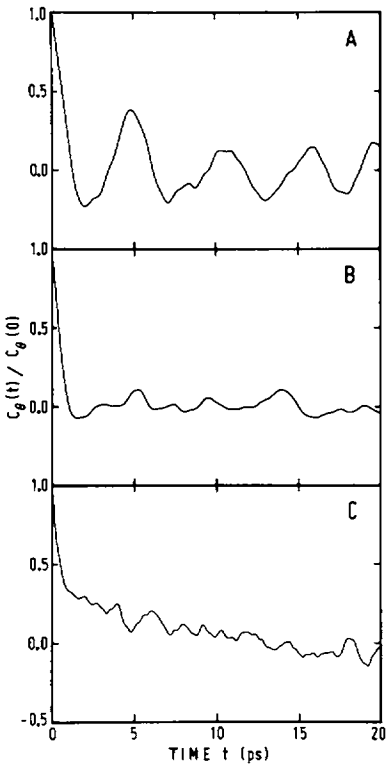

FIGURE 7 Autocorrelation functions $C_\theta(t)$ of the bend angle of the helix for different cases of coupling the helix to the environment, as specified in the legend to Fig. 6.

rounding water molecules increase the damping coefficient for the bend vibration by a factor of 100 relative to the value for weak coupling to a heat bath.

CONCLUSION

The internal dynamics of a 20-residue polyalanine helix was analyzed in terms of autocorrelation functions for the displacement and the velocity of individual atoms, derived from the trajectories of MD simulations. The autocorrelations exhibit oscillations in the range of 50 fs to 5 ps. The fast oscillations correspond to localized vibrations of the bond and dihedral angles, vibrations of the bond lengths do not occur in our MD simulations because the bond lengths were kept constant. The spectrum of the fast oscillations is consistent with experimental data from Raman and infrared spectroscopy. This is not astonishing because as mentioned in the Introduction the parameters of the bonded interactions were chosen to fit these data. Of more interest are the slow oscillations which correspond to delocalized collective vibrations of the helix. They are strongly influenced by the nonbonded interactions whose description lacks a direct experimental justification. To assign the slow oscillations unambiguously to stretch and bend vibrations of the helix, the relative motions of two groups of atoms at the two ends of the helix were analyzed. In this way the 1.4 ps oscillation could be assigned to the stretch vibration and the 4.3 ps oscillation to the bend vibration. The frequency and amplitude of the stretch vibration as well as the deduced elastic modulus of the helix are compatible with experimental data from Raman and infrared spectroscopy, Brillouin scattering, and persistence length measurements. This indicates that the description of the nonbonded interactions is not unrealistic. The description of, for example, the hydrogen bond interaction might even be improved, if more accurate experimental data on the stretch vibration and the elastic modulus become available.

The influence of the environment on the internal dynamics of the helix was studied by coupling the helix to a heat bath or to water. Because the delocalized collective motions are supposed to be more sensitive to the environment than the localized motions, we concentrated our analysis on the collective motions. The frequencies of the stretch and bend vibrations of the helix turned out to be essentially unaffected by the environment, whereas their damping was affected considerably. This implies that the frequencies are determined essentially by the interactions among the helix atoms as expected, whereas the coupling of the helix atoms to the environment determines the damping (25). Water increases the damping of the stretch vibration by a factor of two compared to the case of weak coupling to a heat bath, but the vibration remains underdamped. By contrast, the damping of the bend vibration increases by a factor of 100, it becomes overdamped, i.e., its dynamic behavior changes from oscillation to relaxation. That the bend vibration is more strongly damped by water than the stretch vibration is conceivable. The displacement of the helix ends is much larger for the bend than for the stretch vibration, so that more water molecules have to move away for an oscillation to occur. This overdamping of the bend vibration by water is probably the reason that it is not detected in Raman and infrared measurements. It might be observable as a relaxation process in fluorescence anisotropy decay measurements with picosecond resolution or in microwave absorption measurements. Such experiments would be useful to test the description of damping in the picosecond range by MD simulations. An attempt in that direction has recently been made by measuring the overall rotational diffusion of tryptophan in water and comparing it with the result obtained from an MD simulation (36). Such studies

might be extended to the internal dynamics of peptides and proteins.

Although we could show that the stretch and bend vibration of helices are rather well described in terms of damped harmonic oscillators, such a model does not account for all aspects of these collective motions. Inspection of the fluctuations of the helix length indicates that the polyalanine helix flips randomly between at least two states, one with weakly damped and one with more strongly damped stretch vibrations. Such behavior is reminiscent of chaotic systems with strange attractors (37). More work is required to enlighten this aspect of the dynamic behavior of peptides and proteins.

We thank Olle Edholm for introducing us to Gromos, and for many stimulating discussions. We also thank W. F. van Gunsteren and H. J. C. Berendsen for providing the Gromos program. The cooperativity of R. D. Kloth from this institute, U. Wandel from the Max-Planck-Institut für Biologische Kybernetik, and the staff of the Rechenzentrum Garching is gratefully acknowledged.

Received for publication 14 June 1990 and in final form 21 November 1990.

REFERENCES

1. Frauenfelder, H., F. Parak, and R. D. Young. 1988. Conformational substates in proteins. *Annu. Rev. Biophys. Biophys. Chem.* 17:451–479.
2. Ansari, A., J. Berendzen, S. F. Bowne, H. Frauenfelder, I. E. T. Iben, T. B. Sauke, E. Shyamsunder, and R. D. Young. 1985. Protein states and proteinquakes. *Proc. Natl. Acad. Sci. USA.* 82:5000–5004.
3. Dornmair, K., and F. Jähnig. 1989. Internal dynamics of lactose permease. *Proc. Natl. Acad. Sci. USA.* 86:9827–9831.
4. Tipping, M., K. Viras, and T. A. King. 1984. Low-frequency dynamics of solid poly(L-alanine) from Raman spectroscopy. *Biopolymers.* 23:2891–2899.
5. Fanconi, B., E. W. Small, and W. L. Peticolas. 1971. Phonon dispersion curves and normal coordinate analysis of α-poly-L-alanine. *Biopolymers.* 10:1277–1298.
6. Itoh, K., and T. Shimanouchi. 1970. Vibrational frequencies and modes of α-helix. *Biopolymers.* 9:383–399.
7. Genzel, L., F. Kremer, A. Poglitsch, and G. Bechtold. 1983. Relaxation processes on a picosecond time scale in hemoglobin and poly(L-alanine) observed by millimeter-wave spectroscopy. *Biopolymers.* 22:1715–1729.
8. Cusack, S., J. Smith, J. Finney, B. Tidor, and M. Karplus. 1988. Inelastic neutron scattering analysis of picosecond internal protein dynamics. *J. Mol. Biol.* 202:903–908.
9. Beechem, J. M., and L. Brand. 1985. Time-resolved fluorescence of proteins. *Annu. Rev. Biochem.* 54:43–71.
10. Parak, F., and L. Reinisch. 1986. Mössbauer effect in the study of structure dynamics. *Methods Enzymol.* 131:568–607.
11. Wüthrich, K. 1976. Nuclear magnetic resonance in biological research. Peptides and proteins. North-Holland Publishing Co., Amsterdam.
12. Go, N., T. Noguti, and T. Nishikawa. 1983. Dynamics of a small globular protein in terms of low-frequency vibrational modes. *Proc. Natl. Acad. Sci. USA.* 80:3696–3700.
13. Levy, R. M., and M. Karplus. 1979. Vibrational approach to the dynamics of an α-helix. *Biopolymers.* 18:2465–2495.
14. Karplus, M., and J. A. McCammon. 1983. Dynamics of proteins: elements and function. *Annu. Rev. Biochem.* 53:263–300.
15. Parak, F., and E. W. Knapp. 1984. A consistent picture of protein dynamics. *Proc. Natl. Acad. Sci. USA.* 81:7088–7092.
16. Nadler, W., A. T. Brünger, K. Schulten, and M. Karplus. 1987. Molecular and stochastic dynamics of proteins. *Proc. Natl. Acad. Sci. USA.* 84:7933–7937.
17. Levitt, M. 1982. Protein conformation, dynamics, and folding by computer simulation. *Annu. Rev. Biophys. Bioeng.* 11:251–271.
18. Aqvist, J., W. F. van Gunsteren, M. Leijonmarck, and O. Tapia. 1985. A molecular dynamics study of the C-terminal fragment of the L7/L12 ribosomal protein. *J. Mol. Biol.* 183:461–477.
19. Swaminathan, S., T. Ichiye, W. F. van Gunsteren, and M. Karplus. 1982. Time dependence of atomic fluctuations in proteins: analysis of local and collective motions in bovine pancreatic trypsin inhibitor. *Biochemistry.* 21:5230–5241.
20. Levy, R. M., D. Perahia, and M. Karplus. 1982. Molecular dynamics of an α-helical polypeptide: temperature dependence and deviation from harmonic behavior. *Proc. Natl. Acad. Sci. USA.* 79:1346–1350.
21. Edholm, O., and F. Jähnig. 1988. The structure of a membrane-spanning polypeptide studied by molecular dynamics. *Biophys. Chem.* 30:279–292.
22. Ghosh, I., and J. A. McCammon. 1987. Sidechain rotational isomerization in proteins. *Biophys. J.* 51:637–641.
23. Gilson, M. K., and B. H. Honig. 1986. The dielectric constant of a folded protein. *Biopolymers.* 25:2097–2119.
24. Russell, S. T., and A. Warshel. 1985. Calculations of electrostatic energies in proteins. *J. Mol. Biol.* 185:389–404.
25. Brooks, C. L., and M. Karplus. 1989. Solvent effects on protein motion and protein effects on solvent motion. *J. Mol. Biol.* 208:159–181.
26. Marqusee, S., V. H. Robbins, and R. L. Baldwin. 1989. Unusually stable helix formation in short alanine-based peptides. *Proc. Natl. Acad. Sci. USA.* 86:5286–5290.
27. Berendsen, H. J. C., J. P. M. Postma, W. F. van Gunsteren, A. DiNola, and J. R. Haak. 1984. Molecular dynamics with coupling to an external bath. *J. Chem. Phys.* 81:3684–3690.
28. Ryckaert, J. P., G. Ciccotti, and H. J. C. Berendsen. 1977. Numerical integration of the cartesian equations of motion of a system with constaints: molecular dynamics of n-alkanes. *J. Comp. Phys.* 23:327–341.
29. van Gunsteren, W. F., and M. Karplus. 1982. Effect of constraints on the dynamics of macromolecules. *Macromolecules.* 15:1528–1544.
30. Springer, T. 1972. Quasielastic neutron scattering for the investigation of diffusive motions in solids and liquids. Springer-Verlag, Berlin.
31. Chandrasekhar, S. 1943. Stochastic problems in physics and astronomy. *Rev. Mod. Phys.* 15:1–89.

32. Landau, L. D., and E. M. Lifshitz. 1970. Course of theoretical physics. Vol. 7. Pergamon Press Inc., New York.

33. Peticolas, W. L. 1979. Mean-square amplitudes of the longitudinal vibrations of helical polymers. *Biopolymers.* 18:747–755.

34. Harley, R., D. James, A. Miller, and J. W. White. 1977. Phonons and the elastic moduli of collagen and muscle. *Nature (Lond.).* 267:285–287.

35. Hofmann, H., T. Voss, and K. Kühn. 1984. Localization of flexible sites in thread-like molecules from electron micrographs. *J. Mol. Biol.* 172:325–343.

36. Chen, L. X.-Q., R. A. Engh, and G. R. Fleming. 1988. Reorientation of tryptophan and simple peptides: onset of internal flexibility and comparison with molecular dynamics simulation. *J. Phys. Chem.* 92:4811–4816.

37. Lorenz, E. N. 1963. Deterministic nonperiodic flow. *J. Atmos. Sci.* 20:130–141.